



Cite this: *Chem. Commun.*, 2017, 53, 12822

Received 10th October 2017,
Accepted 3rd November 2017

DOI: 10.1039/c7cc07845e

rsc.li/chemcomm

Long-wavelength fluorescent boronate probes for the detection and intracellular imaging of peroxynitrite†

Adam C. Sedgwick,^a Hai-Hao Han,^b Jordan E. Gardiner,^a Steven D. Bull,^a Xiao-Peng He^b and Tony D. James^a

Two boronate fluorescent probes have been developed for the detection of peroxynitrite (TCFB1 and TCFB2). TCFB1 was shown to have a low sensitivity towards peroxynitrite and have a poor solubility in aqueous solution whereas TCFB2 demonstrated high sensitivity towards peroxynitrite and mitochondria localisation with the ability to detect exogenous and endogenous peroxynitrite in live cells (Hep-G2, RAW 264.7, HeLa and A459).

Peroxynitrite (ONOO[−]) is a highly reactive nitrogen species that is formed *via* the diffusion controlled reaction between superoxide (O₂[−]) and nitric oxide (NO).^{1,2} ONOO[−] acts as a signalling molecule *in vivo* for a number of pathways.^{1,3} However, ONOO[−] is more commonly known for its deleterious properties, causing irreversible damage to a range of biological targets such as lipids, proteins and DNA.⁴ Therefore, ONOO[−] has been implicated as a key pathogenic factor for a number of diseases, which include inflammation, cancer, ischemia-reperfusion and neurodegenerative diseases.^{5–7} In biological systems, ONOO[−] is difficult to measure due to it being short-lived with a half-life ~10–20 ms.¹ Therefore, the development of powerful tools for the detection of ONOO[−] is of significant interest.

With our research, we are particularly interested in the development of small molecule fluorescent probes for the detection of biologically relevant analytes *in vivo* owing to their high sensitivity, selectivity and high spatial and temporal resolution. In the past few years, a number of ONOO[−] fluorescent probes have been developed for imaging in live cells and mice.^{8–13} However, despite significant progress in this area of research, there is a lack of long-wavelength ONOO[−] fluorescent probes. The development of long wavelength/near infrared (NIR) probes is of particular interest because longer excitation/emission wavelengths allows deeper tissue penetration and minimalises

background auto-fluorescence from proteins and photodamage to the biological samples.^{14,15}

In the literature, Sikora *et al.* reported that the reaction rates of ONOO[−] with aromatic boronates are 200 times faster than hypochlorous acid (HOCl/Clo[−]) and a million times faster than hydrogen peroxide (H₂O₂).¹⁶ Therefore, a number of boronate fluorescent probes have been recently developed for the detection of ONOO[−].^{8,17,18}

2-Dicyanomethylene-3-cyano-4,5,5-trimethyl-2,5-dihydrofuran (TCF)-based fluorophores have an internal charge transfer (ICT) donor-π-acceptor (D-π-A) structure with long emission wavelengths. As a result, TCF fluorophores have been used in many applications such as non-linear optic chromophores and molecular probes.^{19–25} With this research, we developed two boronate TCF-based fluorescent probes for the detection of ONOO[−] (TCFB1 and TCFB2). The TCF fluorophore unit was synthesised in one step using the reaction of 3-hydroxy-3-methyl-2-butanone, malonitrile and NaOEt in EtOH. With the TCF unit in hand, the (D-π-A) systems TCFB1 and TCFB2 were isolated in high yield using microwave reaction conditions.²⁶ The microwave irradiation of a mixture of piperidine (Cat.), TCF and 4-(4,4,5,5-tetramethyl-1,3,2-dioxaborolan-2-yl)benzaldehyde in EtOH followed by filtration led to the isolation of the desired TCFB2. For the synthesis of TCFB1, microwave irradiation of a mixture of piperidine (Cat.), TCF and 4-hydroxybenzaldehyde in EtOH followed by filtration led to the isolation of the intermediate TCF-OH. This was subsequently alkylated with 2-(4-(bromomethyl)phenyl)-4,4,5,5-tetramethyl-1,3,2-dioxaborolane using K₂CO₃ and NaI in MeCN to afford TCFB1 in a reasonable yield (47%).



^a Department of Chemistry, University of Bath, Bath, BA2 7AY, UK.

E-mail: t.d.james@bath.ac.uk, s.d.bull@bath.ac.uk

^b Key Laboratory for Advanced Materials & Feringa Nobel Prize Scientist Joint Research Center, East China University of Science and Technology, 130 Meilong Rd., Shanghai 200237, P. R. China. E-mail: xphe@ecust.edu.cn

† Electronic supplementary information (ESI) available. See DOI: 10.1039/c7cc07845e





Fig. 1 Fluorescence spectra of **TCFB1** (10 μM) with addition of ONOO^- (0–100 μM) in PBS buffer solution, 20% DMSO, pH 8.00 at 25 $^{\circ}\text{C}$. λ_{ex} = 560 nm. Slit widths ex = 10 nm and em = 15 nm.

We initially evaluated the UV-Vis (Fig. S2, ESI †) and fluorescence behaviour (Fig. 1 and Fig. S3, ESI †) of **TCFB1**, in pH 8.0 buffer solution (20% DMSO). DMSO was required to improve the aqueous solubility of **TCFB1**. Under these conditions, **TCFB1** produced an up to 6.5-fold fluorescence “turn on” in the presence of ONOO^- (0–100 μM). (Schemes S1, S2 and Fig. S1, ESI †) However, in comparison to our previously reported ESIPT probe, **TCFB1** was less sensitive towards ONOO^- despite a larger “turn on” response.⁸

Subsequently, we evaluated the selectivity of **TCFB1** towards other ROS (Fig. S4, S5 and S11, ESI †). **TCFB1** demonstrated an excellent selectivity for ONOO^- , which permitted the evaluation of its ability to detect exogenous and endogenous ONOO^- in live cells. Unfortunately, due to its poor aqueous solubility, large amounts of precipitate with **TCFB1** was observed (data not shown).

Therefore, we turned our attention towards the evaluation of the UV-Vis and fluorescence properties of **TCFB2**, which has previously been reported for the detection of ClO^- .²⁰ As previously reported for other aryl boronate fluorescent probes,^{27,28} **TCFB2** was found to be initially non-fluorescent with no UV absorption beyond ~ 525 nm (Fig. S6, ESI †). The addition of ONOO^- to **TCFB2** resulted in the appearance of a large emission peak at 606 nm (Fig. 2 and Fig. S7, ESI †). This was accompanied by a colorimetric response (yellow to pink) and the appearance of a large UV absorption peak at ~ 590 nm. **TCFB2** demonstrated high sensitivity and rapid reaction (Fig. S8, ESI †) with ONOO^- and was able to detect very low concentrations (0–10 μM).



Fig. 2 Fluorescence spectra of **TCFB2** (10 μM) with addition of ONOO^- (0–10 μM) in PBS buffer solution, 20% DMSO, pH 8.00 at 25 $^{\circ}\text{C}$. λ_{ex} = 560 nm. Slit widths ex = 10 nm and em = 15 nm.

As predicted, both ClO^- and H_2O_2 also resulted in a fluorescence response (Fig. S9, S10 and S12, ESI †), however, larger concentrations and reaction times were required. These observations clearly demonstrated the greater reactivity of the boronate towards ONOO^- .

Having determined the selectivity of **TCFB2**, we evaluated its ability to image endogenous and exogenous ONOO^- in live cells. **TCFB2** was evaluated in a number of different cell lines (Hep-G2: human hepatoma, HeLa: human cervical cancer, RAW 264.7: mouse macrophage and A549 cells: human lung cancer), which were incubated with **TCFB2** (10 μM) for 30 minutes and washed with PBS buffer solution three times. As shown in Fig. 3, **TCFB2** demonstrated a clear “turn on” response with the addition of Sin-1 (ONOO^- donor). No “turn on” response was observed when the cells were pre-treated with the ONOO^- scavenger uric acid. **TCFB2** also provided a clear “turn on” response for the detection of stimulated ONOO^- . RAW 264.7 cells were used in which ONOO^- was stimulated using lipopolysaccharide (LPS).²⁹ This led to the activation of the **TCFB2** fluorescence intracellularly (Fig. 4). In contrast, no “turn on” response was observed in the presence of uric acid indicating the selectivity for ONOO^- in cells. A cell proliferation assay showed that the compound was not toxic towards all the cell lines used with concentrations well above that used for imaging (Fig. S13, ESI †).

The production of superoxide occurs mainly through the mitochondrial electron transport pathway;³⁰ therefore the mitochondria are the main source of ONOO^- in macrophages. Commercial Mito-tracker Green was used to localise in the mitochondrial compartments of RAW 264.7. We then used **TCFB2** to investigate the subcellular distribution of ONOO^- . The results indicated that the fluorescence of the probe co-localised with that

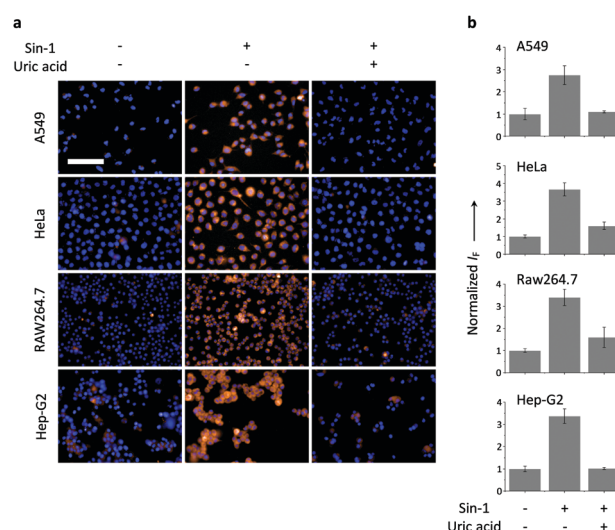


Fig. 3 (a) Fluorescence imaging (scale bar = 100 μm) (b) quantification of different cells incubated with **TCFB2** (10 μM) without (–/–) or with a subsequent addition of Sin-1 (500 μM , a ONOO^- promoter) (+/–) or a subsequent addition of uric acid (100 μM , a ONOO^- quencher) and then Sin-1 (+/+). Excitation and emission wavelengths for **TCFB2** are 560–580 nm and 580–650 nm, respectively. The cell nuclei were stained by Hoechst 33342.





Fig. 4 (a) Fluorescence imaging (scale bar = 100 μm) (b) quantification of RAW 264.7 incubated with **TCFB2** (10 μM) without (–/–) or with a subsequent addition of lipopolysaccharide (LPS, 1 $\mu\text{g mL}^{-1}$) (+/–) or a subsequent addition of both LPS and uric acid (100 μM , a ONOO^- quencher) (+/+). Excitation and emission wavelength for **TCFB2** are 560–580 nm and 580–650 nm, respectively. The cell nuclei were stained by Hoechst 33342.

of the tracker resulting in a Pearson coefficient of 0.84 (Fig. 5). We have also carried out an additional lysosome co-localisation assay, and the result showed that the probe did not co-localise well with lysosome (Pearson's correlation = 0.38) (Fig. S14, ESI[†]). This suggests that ONOO^- was produced at the mitochondria.

In conclusion, we have developed two long-wavelength reaction based fluorescent probes for the detection of ONOO^- . Unfortunately, **TCFB1** had a low solubility in aqueous solution, which led to the observation of precipitates in cell imaging experiments. A glycosylation strategy^{31,32} to improve the water

solubility of the insoluble **TCFB1** is currently underway in our laboratories. However, **TCFB2** displayed selective and sensitive “turn on” with the addition of ONOO^- . The large fluorescence response observed for **TCFB2** facilitated its use in cell imaging experiments. Therefore, **TCFB2** was able to detect exogenous and endogenous ONOO^- with a large fluorescence “turn on” over a range of cell lines (Hep-G2, RAW 264.7, HeLa and A459). Mitochondrial localisation of **TCFB2** was observed by co-localisation with Mito-Tracker Green. Overall, these results demonstrate that **TCFB2** is a useful tool to understand the role of ONOO^- in biological systems and could lead to systems capable of disease diagnosis.

We would like to thank the EPSRC and the University of Bath for funding. A. C. S. and J. E. G. thank the EPSRC for studentships. T. D. J. wishes to thank the Royal Society for a Wolfson Research Merit Award. NMR characterisation facilities were provided through the Chemical Characterisation and Analysis Facility (CCAF) at the University of Bath (www.bath.ac.uk/ccaf). The EPSRC UK National Mass Spectrometry Facility at Swansea University is thanked for analyses. X.-P. He thanks the National Natural Science Foundation of China (21722801 and 21572058), the Science and Technology Commission of Shanghai Municipality (15540723800), the Fundamental Research Funds for the Central Universities (222201717003) and the Shanghai Rising-Star Program (16QA1401400) (to X.-P. He) for financial support. The Catalysis And Sensing for our Environment (CASE) network is thanked for research exchange opportunities. T. D. J. thanks ECUST for a guest professorship. Professors Jia Li and Yi Zang are thanked for their helpful advice on the cellular experiments. All data supporting this study are provided as supplementary information accompanying this paper.

Conflicts of interest

There are no conflicts to declare.

Notes and references

- P. Pacher, J. S. Beckman and L. Liaudet, *Physiol. Rev.*, 2007, **87**, 315.
- J. S. Beckman and W. H. Koppenol, *Am. J. Physiol.: Cell Physiol.*, 1996, **271**, C1424.
- A. Weidinger and A. V. Kozlov, *Biomolecules*, 2015, **5**, 472.
- P. Ascenzi, A. di Masi, C. Sciorati and E. Clementi, *BioFactors*, 2010, **36**, 264.
- H. Ischiropoulos and J. S. Beckman, *J. Clin. Invest.*, 2003, **111**, 163.
- P. Sarchielli, F. Galli, A. Floridi and V. Gallai, *Amino Acids*, 2003, **25**, 427.
- D. A. Wink, Y. Vodovotz, J. Laval, F. Laval, M. W. Dewhirst and J. B. Mitchell, *Carcinogenesis*, 1998, **19**, 711.
- A. C. Sedgwick, X. L. Sun, G. Kim, J. Yoon, S. D. Bull and T. D. James, *Chem. Commun.*, 2016, **52**, 12350.
- Z. N. Sun, H. L. Wang, F. Q. Liu, Y. Chen, P. K. H. Tam and D. Yang, *Org. Lett.*, 2009, **11**, 1887.
- X. Li, R.-R. Tao, L.-J. Hong, J. Cheng, Q. Jiang, Y.-M. Lu, M.-H. Liao, W.-F. Ye, N.-N. Lu, F. Han, Y.-Z. Hu and Y.-H. Hu, *J. Am. Chem. Soc.*, 2015, **137**, 12296.
- F. B. A. Yu, P. Li, G. Y. Li, G. J. Zhao, T. S. Chu and K. L. Han, *J. Am. Chem. Soc.*, 2011, **133**, 11030.
- F. B. Yu, P. Li, B. S. Wang and K. L. Han, *J. Am. Chem. Soc.*, 2013, **135**, 7674.
- D. Cheng, Y. Pan, L. Wang, Z. B. Zeng, L. Yuan, X. B. Zhang and Y. T. Chang, *J. Am. Chem. Soc.*, 2017, **139**, 285.



Fig. 5 (a) Fluorescence co-localisation of **TCFB2** (10 μM) with Mito-Tracker Green (1 μM) in RAW 264.7 cells (scale bar = 20 μm). (b) Fluorescence quantification of **TCFB2** and Mito-Tracker of a selected section (the black line in “Merged” panel) of a RAW 264.7 cell. Excitation wavelength for Mito-Tracker Green and **TCFB2** is 489 and 579 nm, respectively. Emission wavelength for Mito-Tracker Green and **TCFB2** is 506 and 603 nm, respectively. The cell nuclei were stained by Hoechst 33342.



- 14 L. Yuan, W. Y. Lin, K. B. Zheng, L. W. He and W. M. Huang, *Chem. Soc. Rev.*, 2013, **42**, 622.
- 15 R. Weissleder, *Nat. Biotechnol.*, 2001, **19**, 316.
- 16 A. Sikora, J. Zielonka, M. Lopez, J. Joseph and B. Kalyanaraman, *Free Radical Biol. Med.*, 2009, **47**, 1401.
- 17 X. Sun, Q. Xu, G. Kim, S. E. Flower, J. P. Lowe, J. Yoon, J. S. Fossey, X. Qian, S. D. Bull and T. D. James, *Chem. Sci.*, 2014, **5**, 3368.
- 18 S. Palanisamy, P. Y. Wu, S. C. Wu, Y. J. Chen, S. C. Tzou, C. H. Wang, C. Y. Chen and Y. M. Wang, *Biosens. Bioelectron.*, 2017, **91**, 849.
- 19 Y. H. Yang, J. L. Liu, H. Y. Xiao, Z. Zhen and S. H. Bo, *Dyes Pigm.*, 2017, **139**, 239.
- 20 W. Shu, L. G. Yan, Z. K. Wang, J. Liu, S. Zhang, C. Y. Liu and B. C. Zhu, *Sens. Actuators, B*, 2015, **221**, 1130.
- 21 Y. J. Wang, Y. Shi, Z. Y. Wang, Z. F. Zhu, X. Y. Zhao, H. Nie, J. Qian, A. J. Qin, J. Z. Sun and B. Z. Tang, *Chem. – Eur. J.*, 2016, **22**, 9784.
- 22 Y. R. Wang, L. Feng, L. Xu, Y. Li, D. D. Wang, J. Hou, K. Zhou, Q. Jin, G. B. Ge, J. N. Cui and L. Yang, *Chem. Commun.*, 2016, **52**, 6064.
- 23 B. C. Zhu, H. Kan, J. K. Liu, H. G. Liu, Q. Wei and B. Du, *Biosens. Bioelectron.*, 2014, **52**, 298.
- 24 C. Y. Li, M. Li, Y. Li, Z. S. Shi, Z. J. Li, X. B. Wang, J. Sun, J. W. Sun, D. M. Zhang and Z. C. Cui, *J. Mater. Chem. C*, 2016, **4**, 8392.
- 25 T. Yu, G. X. Yin, P. Yin, Y. Zeng, H. T. Li, Y. Y. Zhang and S. Z. Yao, *RSC Adv.*, 2017, **7**, 24822.
- 26 M. Ipu, C. Billon, G. Micouin, J. Samarut, C. Andraud and Y. Bretonniere, *Org. Biomol. Chem.*, 2014, **12**, 3641.
- 27 E. W. Miller, A. E. Albers, A. Pralle, E. Y. Isacoff and C. J. Chang, *J. Am. Chem. Soc.*, 2005, **127**, 16652.
- 28 B. C. Dickinson, C. Huynh and C. J. Chang, *J. Am. Chem. Soc.*, 2010, **132**, 5906.
- 29 A. Vazquez-Torres, J. Jones-Carson and E. Balish, *Infect. Immun.*, 1996, **64**, 3127.
- 30 M. D. Brand, C. Affourtit, T. C. Esteves, K. Green, A. J. Lambert, S. Miwa, J. L. Pakay and N. Parker, *Free Radical Biol. Med.*, 2004, **37**, 755.
- 31 X.-P. He, Y. Zang, T. D. James, J. Li, G.-R. Chen and J. Xie, *Chem. Commun.*, 2017, **53**, 82.
- 32 J. Zhang, Y. Fu, H.-H. Han, Y. Zang, J. Li, X.-P. He, B. L. Feringa and H. Tian, *Nat. Commun.*, 2017, **8**, 987.

